

Electronic Structure of Ni Complexes by X-ray Resonance Raman Spectroscopy (Resonant Inelastic X-ray Scattering)

Pieter Glatzel,^{*,†} Uwe Bergmann,^{†,‡} Weiwei Gu,[†] Hongxin Wang,[†] Sergey Stepanov,[§] Beaven S. Mandimutsira,^{||} Charles G. Riordan,^{||} Colin P. Horwitz,[⊥] Terry Collins,[⊥] and Stephen P. Cramer^{*,†,‡}

Department of Applied Science, University of California, Davis, California 95616, Lawrence Berkeley National Laboratory, Berkeley, California 94720, BioCAT at the Advanced Photon Source, Argonne National Laboratory, Argonne, Illinois 60439, Department of Chemistry, University of Delaware, Newark, Delaware 19716, and Department of Chemistry, Carnegie-Mellon University, Pittsburgh, Pennsylvania 15213

Received February 25, 2002

Conventional resonance Raman spectroscopy (RRS) is a well-established technique that uses UV–visible radiation to probe the vibrational properties of chromophores.¹ In this communication, we present results with the related technique of X-ray resonance Raman spectroscopy or resonant inelastic X-ray scattering (RIXS). We illustrate the potential of this technique with a study of Ni compounds, using excitation at the K (1s) absorption edge and fluorescence detection of the subsequent 2p to 1s transition. We show that this method combines the merits of both hard X-ray K-edge² (1s) and soft X-ray L-edge³ (2p) absorption spectroscopy.

In the two-step model for 1s2p RIXS,⁴ an incident photon with energy Ω promotes a 1s electron into an unoccupied molecular orbital. A 2p electron fills the 1s vacancy and emits a photon with energy ω . Although both incident and emitted photons lie in the hard X-ray range (>5 keV), the final states of the system exhibit the same 2p vacancy encountered in L-edge soft X-ray spectroscopy. This is illustrated for a “1s \rightarrow 3d” resonance in Figure 1. The intensities and splittings of the spectral features in 1s2p RIXS can be described theoretically by the same Kramers–Heisenberg equation used to describe the UV–visible RRS.⁵ The intermediate state with a 1s core hole is reached from the electronic ground state via the dipole or the quadrupole operator. The decay of the 1s hole occurs via the dipole operator into the final state with a 2p vacancy.

Several intermediate and final states can be reached. The splittings and relative intensities of the transitions between the different states contain chemical information which can be displayed in a contour plot, where the two axes are the incident energy Ω and the energy transfer $\Omega - \omega$. The energy transfer or loss $\Omega - \omega$ (final-state energy) scale corresponds with the excitation energy in L-edge spectra (Figure 1), and we obtain L₃ (2p_{3/2})- and L₂ (2p_{1/2})-like spectra by projections along constant incident energy Ω . The natural line width in this case is the same as in L-edge spectroscopy, thus overcoming the short 1s core hole lifetime that considerably broadens the K-edge spectral features.⁶ Although the K-edge lifetime still pertains to Ω scans (constant final-state energy $\Omega - \omega$), the reduction in overlapping features yields an effective sharpening in this dimension as well.

Figure 2 illustrates the properties of 1s2p RIXS for Ni in various spin and oxidation states.^{7,10} In these contour plots, the intensities

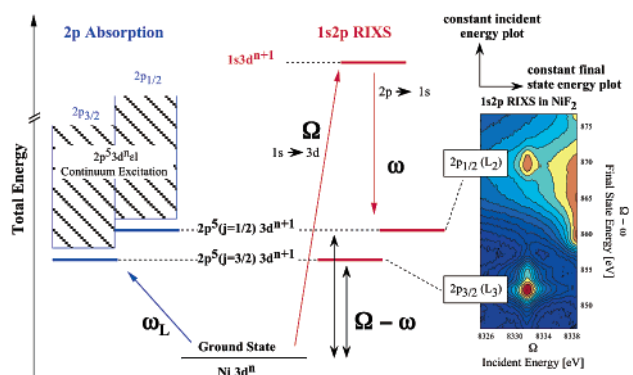


Figure 1. Energy scheme for 1s2p RIXS compared to L-edge absorption spectroscopy. A 1s2p RIXS contour plot for NiF₂ is shown as an example, and the two line plots that we extract from the contour plots are illustrated. The photon energies are denoted ω_L (L-edge), Ω (K-edge), and ω (inelastically scattered).

(on logarithmic scales) are expressed as different colors. Isolated resonant excitations appear as islands along a diagonal in the plots with tails extending parallel to the Ω and $\Omega - \omega$ axes. With increasing excitation energy, the resonances turn into continuum excitations. We focus on the “preedge” excitation region that involves the lowest unoccupied molecular orbitals and on final states with 2p_{3/2} vacancies (L₃-edge).

By traversing the contour plots along lines of constant $\Omega - \omega$, one obtains excitation spectra for constant final-state energy (Figure 3).¹¹ The weak 1s \rightarrow 3d resonances are now separated from the strong dipole allowed transitions at higher energies. The shifts of the 1s \rightarrow 3d resonances with oxidation state are clearly visible. The Ni(I) complex has one vacant 3d orbital; accordingly, we only observe one 1s \rightarrow 3d resonance. For Ni(II), there is either a single vacant 3d orbital (low-spin) or a pair of nearly degenerate 3d orbitals (high-spin); again, we see only a single 1s \rightarrow 3d resonance. In contrast, two 1s \rightarrow 3d resonances are observed for the Ni(III) complex. This is consistent with at least some 3d⁷ character in the ground-state configuration. Here, the Ni site has approximately tetragonal symmetry, and the low-spin ($S = 1/2$) configuration yields one unoccupied 3d_{x²-y²} orbital and a half-filled 3d_{xy} orbital.¹⁰ These features are nearly invisible in the transmission spectrum.

Traversing the contour plots parallel to $\Omega - \omega$ at a fixed excitation energy Ω yields “energy-loss” spectra that involve the same final states as in 2p \rightarrow 3d (L_{2,3}) absorption spectroscopy (Figure 3).¹² In the following, we discuss the 2p_{3/2} (L₃) structure

* To whom correspondence should be addressed. E-mail: SPCramer@ucdavis.edu; PGlatzel@lbl.gov.

† University of California, Davis.

‡ Lawrence Berkeley National Laboratory.

§ BioCAT at the Advanced Photon Source, Argonne National Laboratory.

|| University of Delaware.

⊥ Carnegie-Mellon University.

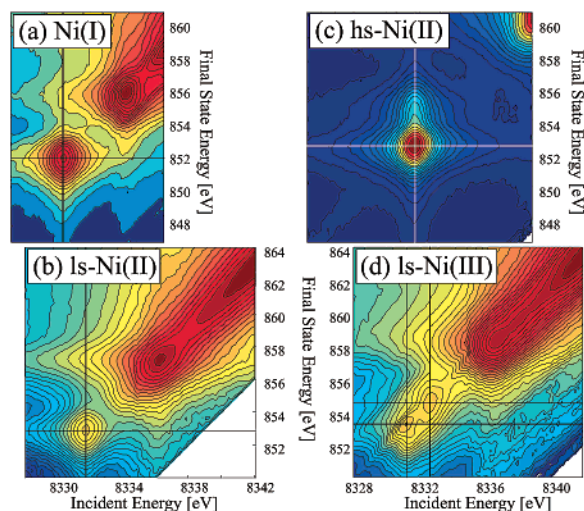


Figure 2. Contour plots for Ni coordination complexes: (a) Ni(I) in $[\text{PhTb}^{\text{Bu}}]\text{NiCO}$, (b) Ni(II) low-spin (ls) in $(\text{Ph}_4\text{As})_2\text{Ni}(\text{S}_2\text{C}_2(\text{CF}_3)_2)_2$, (c) Ni(II) high-spin (hs) in NiF_2 , and (d) Ni(III) low-spin in $[\text{Ni}(\eta^4\text{-DEMAMPA-DCB})]^-$. The vertical (constant incident energy) and horizontal (constant final-state energy) lines correspond to the line plots shown in Figure 3.

below 855.5 eV final-state energy. In this case, exciting the $1s \rightarrow 3d$ intermediate resonance of the Ni(I) complex yields final states with a $2p^5 3d^{10}$ configuration. The energy loss spectrum does not show any splitting because of the filled 3d shell. Within the experimental resolution, a symmetrical peak is also observed for low-spin Ni(II). In contrast, the high-spin Ni(II) and low-spin Ni(III) L_3 energy-loss spectra exhibit asymmetries due to multiplet structure.¹³ These features arise from $(2p,3d)$ and $(3d,3d)$ Coulomb and exchange interactions. Additional structures arise from orbital energy splittings in the case of Ni(III). Multiplet splitting yields information on the valence and spin state of the metal center, and various L-edge studies have used these features to characterize metal centers.³ Specifically, in L-edge spectroscopy, the high-energy shoulder in the L_3 line has been used as a diagnostic of high-spin Ni(II) in metalloproteins,¹⁴ while a low-energy peak ascribed to Ni(III) has been used to characterize Ni oxides.¹⁵ The energy-loss spectra show features above the $2p_{3/2}$ structure. Comparison with Figure 2 shows that the intensity of these features arises from resonances at higher incident energies.

In summary, we have demonstrated the potential of $1s2p$ RIXS spectroscopy for characterization of Ni complexes. By extension, this approach should be applicable to a wide range of transition metals, as well as final states with 3p or valence electron excitations. The $1s2p$ RIXS enables to separate out the lowest K-edge resonances (preedge features). It potentially offers the resolution of L-edge soft X-ray spectroscopy in the energy loss spectra combined with the bulk sensitivity of hard X-rays. The line widths in the RIXS energy-loss spectra reported here are broadened by instrumental resolution. Improvements in X-ray optics will remove this limitation. The sensitivity of RIXS is high enough to examine transition metals in metalloproteins. This technique promises to be a valuable probe of electronic structure.

Acknowledgment. This work was supported by the National Institutes of Health Grants GM-44380 and the DOE Office of Biological and Environmental Research. Use of the Advanced Photon Source was supported by the U.S. Department of Energy, Basic Energy Sciences, Office of Science, under Contract No. W-31-109-ENG-38. BioCAT is a National Institutes of Health-

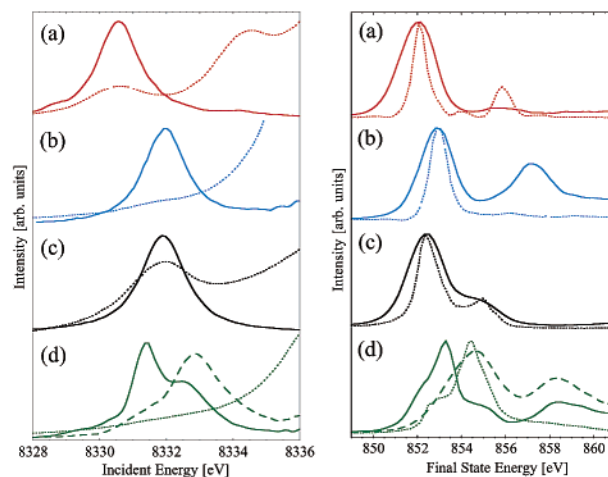


Figure 3. Conventional absorption spectra (dotted lines) compared to RIXS line plots (solid/dashed lines) as indicated in Figure 2 for the four Ni coordination complexes. (Left panel) K-preedge absorption spectra and RIXS constant final-state energy plots. (Right panel) L_3 -edge absorption spectra and RIXS constant incident energy or energy-loss plots.

supported Research Center RR-08630. The ALS and SSRL are supported by the Department of Energy, Office of Basic Energy Sciences.

References

- (1) (a) Czernuszewicz, R. S.; Spiro, T. G. *IR, Raman, and Resonance Raman Spectroscopy*; Solomon, E. I., Lever, A. B. P., Eds.; John-Wiley & Sons: New York, 1999; Vol. 1, pp 353–441. (b) Solomon, E. I.; Hanson, M. A. *Bioinorganic Spectroscopy*; Solomon, E. I., Lever, A. B. P., Eds.; John-Wiley & Sons: New York, 1999; Vol. 2, pp 1–129.
- (2) Solomon, E. I.; Hodgson, K. O. *Spectroscopic Methods in Bioinorganic Chemistry*; Division of Inorganic Chemistry; American Chemical Society Meeting; American Chemical Society (Distributed by Oxford University Press): Washington, DC, New York, 1998.
- (3) de Groot, F. M. F. *J. Electron Spectrosc. Relat. Phenom.* **1994**, *676*, 529–622.
- (4) Caliebe, W. A.; Kao, C. C.; Hastings, J. B.; Taguchi, M.; Uozumi, T.; de Groot, F. M. F. *Phys. Rev. B* **1998**, *58*, 13452–13458.
- (5) (a) Carra P.; Fabrizio, M.; Thole, B. T. *Phys. Rev. Lett.* **1995**, *47*, 3000–3003. (b) Kotani, A.; Shin, S. *Rev. Mod. Phys.* **2001**, *73*, 203–46.
- (6) de Groot, F. M. F. *Chem. Rev.* **2001**, *101*, 1779–1808.
- (7) The RIXS spectra were recorded at the Bio-CAT beamline at the Advanced Photon Source (APS).⁸ The incident beam monochromator used a pair of Si(400) crystals, and the energy bandwidth at 8330 eV was 1.0 eV. Radiation damage studies were performed on each sample. The fluorescence spectrometer for the current experiments used three 8.9-cm diameter Si(620) analyzer crystals.⁹ The fluorescence spectrometer energy bandwidth was approximately 0.8 eV at 7478 eV.
- (8) Bunker, G. B.; Irving, T.; Black, E.; Zhang, K.; Fischetti, R.; Wang, S.; Stepanov, S. *Synchrotron Radiation Instrumentation: Tenth US National Conference: Ithaca, New York, June 1997*; Fontes, E., Ed.; American Institute of Physics: Woodbury, NY, 1997; p 16.
- (9) Bergmann, U.; Cramer, S. P. *Proc. SPIE-Int. Soc. Opt. Eng.* **1998**, *3448*, 198–209.
- (10) NiF_2 was used as received from Aldrich. For the Ni(II) low-spin complex, see: (a) Davison, A.; Holm, R. H. *Inorg. Synth.* **1967**, *10*, 8–26. (b) Wang, K.; McConnachie, J. M.; Stiefel, E. I. *Inorg. Chem.* **1999**, *38*, 4334–4341. For the Ni(I) complex, see: (c) Schebler, P. J.; Mandimutsira, B. S.; Riordan, C. G.; Liable-Sands, L. M.; Incarvito, C. D.; Rheingold, A. L. *J. Am. Chem. Soc.* **2001**, *123*, 331–332. For the Ni(III) complex, see: (d) Uffelman, E. S. Ph.D. Thesis, California Institute of Technology, 1992.
- (11) Conventional K-edge absorption spectra were recorded at SSRL beamline 7-3 using a water-cooled Si(220) double crystal monochromator with an energy bandwidth of ~ 1.0 eV.
- (12) L-edge absorption spectra were recorded at the ALS undulator beamline 4.0.2. The calculated energy bandwidth is 0.3 eV at 850 eV.
- (13) Slater, J. C. *Quantum Theory of Atomic Structure*; McGraw-Hill: New York, 1960.
- (14) Wang, H. X.; Ralston, C. Y.; Patil, D. S.; Jones, R. M.; Gu, W.; Verhagen, M.; Adams, M.; Ge, P.; Riordan, C.; Marganian, C. A.; Mascharak, P.; Kovacs, J.; Miller, C. G.; Collins, T. J.; Brooker, S.; Croucher, P. D.; Wang, K.; Stiefel, E. I.; Cramer, S. P. *J. Am. Chem. Soc.* **2000**, *122*, 10544–10552.
- (15) Hu, Z.; Kaindl, G.; Warda, S. A.; Reinen, D.; deGroot, F. M. F.; Müller, B. G. *Chem. Phys.* **1998**, *232*, 63–74.

JA026028N